



## Molecular requirements involving the human platelet protease-activated receptor-4 mechanism of activation by peptide analogues of its tethered-ligand

I. C. Moschonas, T. F. Kellici, T. Mavromoustakos, P. Stathopoulos, V. Tsikaris, V. Magafa, A. G. Tzakos & A. D. Tselepis


To cite this article: I. C. Moschonas, T. F. Kellici, T. Mavromoustakos, P. Stathopoulos, V. Tsikaris, V. Magafa, A. G. Tzakos & A. D. Tselepis (2017) Molecular requirements involving the human platelet protease-activated receptor-4 mechanism of activation by peptide analogues of its tethered-ligand, *Platelets*, 28:8, 812-821, DOI: [10.1080/09537104.2017.1282607](https://doi.org/10.1080/09537104.2017.1282607)



To link to this article: <https://doi.org/10.1080/09537104.2017.1282607>

 View supplementary material 

 Published online: 07 Mar 2017.

 Submit your article to this journal 

 Article views: 202




 View related articles 

 View Crossmark data 

 Citing articles: 1 View citing articles 

## ORIGINAL ARTICLE

# Molecular requirements involving the human platelet protease-activated receptor-4 mechanism of activation by peptide analogues of its tethered-ligand

I. C. Moschonas<sup>1</sup>, T. F. Kellici <sup>2,3</sup>, T. Mavromoustakos <sup>3,4</sup>, P. Stathopoulos<sup>2</sup>, V. Tsikaris<sup>2</sup>, V. Magafa<sup>5</sup>, A. G. Tzakos <sup>2</sup>, & A. D. Tselepis<sup>1</sup>

<sup>1</sup>Atherothrombosis Research Centre/Laboratory of Biochemistry, Department of Chemistry, University of Ioannina, Ioannina, Greece, <sup>2</sup>Sector of Organic Chemistry and Biochemistry, Department of Chemistry, University of Ioannina, Ioannina, Greece, <sup>3</sup>Department of Chemistry, National and Kapodistrian University of Athens, Panepistimiopolis Zografou, Athens, Greece, <sup>4</sup>Department of Chemistry, York College and the Graduate Center of the City University of New York, Jamaica, NY, USA, and <sup>5</sup>Laboratory of Pharmacognosy and Chemistry of Natural Products, Department of Pharmacy, University of Patras, Patras, Greece

## Abstract

Thrombin is the most potent agonist of human platelets and its effects are primarily mediated through the protease-activated receptors (PARs)-1 and -4. Although PAR-1 has higher affinity for thrombin than PAR-4, both receptors contribute to thrombin-mediated actions on platelets. Recently, a potent and selective PAR-1 antagonist (vorapaxar) was approved for clinical use in selected patients. In contrast, despite the fact that several PAR-4 antagonists have been developed, few of them have been tested in clinical trials.

The aim of the present study was to elucidate the molecular requirements involving the PAR-4 mechanism of activation by peptide analogues of its tethered-ligand.

Eight synthetic PAR-4 tethered-ligand peptide analogues were synthesized and studied for their agonistic/antagonistic potency and selectivity toward human washed platelet aggregation, using light transmittance aggregometry. In addition, *in silico* studies were conducted to describe the receptor–peptide interactions that are developed following PAR-4 exposure to the above analogues. To provide a first structure-activity relationship rationale on the bioactivity profiles recorded for the studied analogues, molecular docking was applied in a homology model of PAR-4, derived using the crystal structure of PAR-1.

The following peptide analogues were synthesized: AYPGKF-NH<sub>2</sub> (1), GYPGKF-NH<sub>2</sub> (2), Ac-AYPGKF-NH<sub>2</sub> (3), *trans*-cinnamoyl-AYPGKF-NH<sub>2</sub> (4), YPGKF-NH<sub>2</sub> (5), Ac-YPGKF-NH<sub>2</sub> (6), *trans*-cinnamoyl-YPGKF-NH<sub>2</sub> (7), and *caffeoyl*-YPGKF-NH<sub>2</sub> (8). Peptide (1) is a selective PAR-4 agonist inducing platelet aggregation with an IC<sub>50</sub> value of 26.2 μM. Substitution of Ala-1 with Gly-1 resulted in peptide (2), which significantly reduces the agonistic potency of peptide (1) by 25-fold. Importantly, substitution of Ala-1 with *trans*-cinnamoyl-1 resulted in peptide (7), which completely abolishes the agonistic activity of peptide (1) and renders it with a potent antagonistic activity toward peptide (1)-induced platelet aggregation. All other peptides tested were inactive. Tyr-2, residue, along with its neighboring environment was a key determinant in the PAR-4 recognition mode. When the neighboring residues to Tyr-2 provided an optimum spatial ability for the ligand to enter into the binding site of the transmembrane receptor, a biological response was propagated. These results were compared with the predicted binding poses of small molecule antagonists of PAR-4, denoted as YD-3, ML-354, and BMS-986120. π–π stacking interaction with Tyr-183 appears to be critical and common for both small molecules antagonists and the peptide *trans*-cinnamoyl-YPGKF-NH<sub>2</sub>.

Conclusively, the lipophilicity, size, and aromatic nature of the residue preceding Tyr-2 are determining factors on whether a human platelet PAR-4 tethered-ligand peptide analogue will exert an agonistic or antagonistic activity.

## Keywords

Peptides, platelets, protease-activated receptors, thrombin, vorapaxar

## History

Received 1 September 2016

Revised 12 December 2016

Accepted 6 January 2017

Published online 6 March 2017

Correspondence: Alexandros D. Tselepis, Atherothrombosis Research Centre/Department of Chemistry, University of Ioannina, 45110 Ioannina, Greece. Tel: (+30) 26510-08365; Fax: (+30) 26510-08785; E-mail: [atselep@uoi.gr](mailto:atselep@uoi.gr)

Color versions of one or more of the figures in the article can be found online at [www.tandfonline.com/iplt](http://www.tandfonline.com/iplt).

## Introduction

Platelets are crucial for normal hemostasis and thrombosis. Thrombin is the most potent platelet activator [1,2] and in humans mediates its actions through protease-activated receptors (PARs)-1 and -4 [3]. PARs constitute a subset of four G protein-coupled receptors (GPCRs), designated PAR-1 to -4, which are activated by serine proteases, utilizing a unique mechanism which requires proteolysis unmasking their

extracellular *N*-terminal domain. The latter event leads to the formation of a new *N*-terminus, called the “tethered-ligand”, which binds intramolecularly to the receptor and induces the signaling cascade [4]. Alternatively, synthetic peptides, based on the tethered-ligand sequence, can function as exogenous agonists or antagonists, with no interference of the aforementioned proteolytic mechanism. Such agonists have been used widely until today and include thrombin-receptor activating peptide-6 (TRAP-6; sequence SFLLRN-NH<sub>2</sub> [5]) and PAR-4 activating peptide (PAR-4-AP; sequence AYPGKF-NH<sub>2</sub> [6]).

PAR-1 is considered the primary thrombin receptor in platelets, due to its higher thrombin affinity. However, when the two receptors are co-expressed, the difference between PAR-1 and -4 affinities for thrombin is not substantial [7]. This may be due to the formation of a PAR-1/-4 heterodimer [7,8] upon platelet thrombin exposure [9]. There is evidence suggesting that the PAR-1/-4 complex is critical for proper platelet activation by thrombin: PAR-1 mediates a brief G<sub>q</sub> signal initiating the aggregation process, which is weak and reversal. In the meantime, it acts as a co-factor for PAR-4 activation, while thrombin is still bound to PAR-1. When PAR-4 is activated, it triggers a prolonged G<sub>q</sub> signal that complements the cascade of PAR-1 and renders the aggregation irreversible [10].

PAR-1 pharmacology has been prompted rapidly, resulting in vorapaxar (Zontivity<sup>®</sup>, Merck & Co.), a potent, selective and competitive, oral PAR-1 antagonist [11]. Several PAR-4 antagonists have been developed, however only few of them have been studied in clinical settings. These antagonists include: (a) tethered-ligand peptide analogues, (b) pepducins, and (c) heterocyclic molecules with an indazole or indole core. Tethered-ligand peptide analogues are hexapeptides that bind to the extracellular part of PAR-4 and prevent proper receptor activation by thrombin or an exogenous agonist. They are relatively weak antagonists, as they require about 400 μM to achieve inhibition of aggregation by 80%. Two peptides of this category have been described until now, *trans*-cinnamoyl-YPGKF-NH<sub>2</sub> and *trans*-cinnamoyl-APGKF-NH<sub>2</sub> [12–14].

The aim of the present study was to elucidate in greater detail the molecular requirements involving the PAR-4 mechanism of activation. In this regard, we synthesized eight PAR-4 tethered-ligand peptide analogues and tested their effect on platelet aggregation. Furthermore, the selectivity of the most potent agonistic analogue toward PAR-4 versus PAR-1 was evaluated. In addition, *in silico* studies were conducted to describe the receptor-peptide interactions that are developed following PAR-4 exposure to the above analogues. These *in silico* studies were complemented with the predicted binding poses of the three small organic molecule antagonists of PAR-4, symbolized as YD-3 [15], ML-354 [16], and BMS-986120 [17].

## Materials and methods

### Reagents

Triisopropylsilane (TIS), 1,2-ethanedithiol (EDT), *N,N*-diisopropyl ethyl amine (DIEA), trifluoroacetic acid (TFA), 1,3-dimethoxybenzene (DMB), and piperidine were Merck-Schuchardt (Darmstadt, Germany) products and used without further purification. Apyrase and prostaglandin E<sub>1</sub> (PGE<sub>1</sub>) were purchased from Sigma-Aldrich (Saint-Louis, MO, USA). TRAP-6 was purchased from Bachem (Bubendorf, Switzerland). Vorapaxar was purchased from Axon MedChem (Groningen, Netherlands).

## Peptide synthesis, purification, and characterization

All peptides presented in this work were synthesized manually, with standard Fmoc  $\alpha$ -protection [18] on Rink Amide. Fmoc amino acid derivatives, 2-(1*H*-benzotriazol-1-yl)-1,1,3,3-tetramethyluronium hexafluorophosphate (HBTU), and 1-Hydroxybenzotriazole (HOBt) 4-(2',4'-dimethoxy phenyl-Fmoc-aminomethyl)-phenoxy-linked polystyrene (Rink amide) and 4-(hydroxymethyl) phenoxy-methyl-linked polystyrene (Wang) were from GL Biochem (Shanghai). Amino acids were introduced bearing Fmoc-protection as also appropriate protecting groups in the side chain. Fmoc deprotection steps were carried out with 20% piperidine in DMF (v/v) for 15 min. Coupling reactions of Fmoc amino acids were performed in DMF, using a molar ratio of amino acid/HBTU/HOBt/DIEA/resin (3:3:3:6:1). Reactions were monitored with the color Kaiser test [19]. It followed the placement of the dry peptide resin using classical cleavage mixture [20]. After 3 h stirring, the resin was filtered and washed with TFA. The combined filtrates were concentrated under reduced pressure. Hexane was added and the resulted solution was re-concentrated. This procedure was performed twice. The peptide was precipitated with cold diethyl ether, filtered, dissolved in 2 N acetic acid, and lyophilized. The following peptide analogs were synthesized: AYPGKF-NH<sub>2</sub> (1), GYPGKF-NH<sub>2</sub> (2), Ac-AYPGKF-NH<sub>2</sub> (3), *trans*-cinnamoyl-AYPGKF-NH<sub>2</sub> (4), YPGKF-NH<sub>2</sub> (5), Ac-YPGKF-NH<sub>2</sub> (6), *trans*-cinnamoyl-YPGKF-NH<sub>2</sub> (7), and *caffeoyl*-YPGKF-NH<sub>2</sub> (8) (Table I). All peptides were purified with RP-HPLC. The peptides were characterized by analytical HPLC and LC/Electrospray Mass Spectrometry (ESI-MS) analysis and were found to be > 99% pure. LC/MS experiments were performed on a quadrupole ion-trap mass analyzer (Agilent Technologies, model MSD trap SL) retrofitted to a 1,100 binary HPLC system equipped with a degasser, autosampler, diode array detector, and electrospray ionization source (Agilent Technologies, Karlsruhe, Germany).

## Preparation of washed human platelets

Washed platelets were prepared from citrated whole blood obtained from non-smoking, apparently healthy volunteers who denied ingesting any antithrombotic and anti-inflammatory agents for at least two weeks prior to venipuncture, as previously described [21,22]. Briefly, whole blood containing 0.1 U/mL apyrase and 1 μM PGE<sub>1</sub> was centrifuged at 126 × *g* for 15 min to obtain platelet-rich plasma (PRP). The PRP was diluted with

Table I. Numbers, structure, and effect on washed platelet aggregation of the peptides studied.

Peptide Number	Structure	Effect on platelets	EC <sub>50</sub> /IC <sub>50</sub> values (μM)
(1)	AYPGKF-NH <sub>2</sub>	Agonist	26.2
(2)	GYPGKF-NH <sub>2</sub>	Agonist	657.0
(3)	Ac-AYPGKF-NH <sub>2</sub>	Inactive	-
(4)	<i>trans</i> -cinnamoyl-AYPGKF-NH <sub>2</sub>	Inactive	-
(5)	YPGKF-NH <sub>2</sub>	Inactive	-
(6)	Ac-YPGKF-NH <sub>2</sub>	Inactive	-
(7)	<i>trans</i> -cinnamoyl-YPGKF-NH <sub>2</sub>	Antagonist toward peptide (1)	69.4
(8)	<i>caffeoyl</i> -YPGKF-NH <sub>2</sub>	Inactive	-
TRAP-6	SFLLRN	Agonist	6.8

Values represent the mean from at least three different platelet preparations.

Abbreviations: TRAP-6 = thrombin-receptor activating peptide-6.

washing buffer pH = 6.5, 0.015 U/mL apyrase and 0.1  $\mu\text{M}$  PGE<sub>1</sub> and centrifuged at  $975 \times g$  for 12 min. The resulting platelet pellet was re-suspended in washing buffer, 0.015 U/mL apyrase, and 0.1  $\mu\text{M}$  PGE<sub>1</sub>. After a second centrifugation at  $975 \times g$  for 12 min, the pellet was re-suspended using suspension buffer pH = 7.35. Platelets were counted using a hemocytometer, adjusted to a final concentration of  $2.5 \times 10^8 \text{ mL}^{-1}$  using suspension buffer and supplemented with 1 mM calcium chloride.

### Light transmittance aggregometry

Light transmittance aggregometry (LTA) was performed using a Chrono-Log Lumi-Aggregometer model 700-4DR (Havertown, PA, USA) with the AggroLink software package. Washed platelet aliquots of 0.5 mL were incubated at 37°C under stirring conditions (1,200 rpm) for 1 min before the addition of each agonistic peptide (or its vehicle). In order to evaluate the antagonistic activity of each peptide or vorapaxar, washed platelet aliquots were incubated for 3 min at 37°C with each antagonist (or its vehicle; DMSO) before the addition of the agonistic peptide. All synthetic peptides were tested at various concentrations up to 1 mM, TRAP-6 was used at concentrations of 10–20  $\mu\text{M}$ , whereas vorapaxar in DMSO was tested at concentrations ranging from 0.1 nM to 1.25  $\mu\text{M}$ . Aggregation was expressed as the maximum percentage change in light transmittance from baseline achieved within 5 min after addition of agonist, using suspension buffer as reference. All LTA assays were conducted within 3 h after venipuncture.

### In silico studies

#### Amino acid sequence for PAR-4 and its alignment

The UniProt database [23], was used to identify the amino acid sequence for human PAR-4. Homologs for this GPCR were screened in NCBI PDB database using the “PSI-BLAST homology search” option in Prime 4.0 [24] to identify the highest identity protein structure. The structure with the highest sequence identity and best BLAST bit score was the crystal structure of PAR-1 (PDB ID: 3VW7 [25]). The alignment of the two sequences was generated using Prime STA, a program best used for cases of medium sequence identity, and selected the GPCR-specific alignment [26].

#### Model building for PAR-4, refinement, and validation

For the construction of the model, the energy-based model building method was chosen. In this method, the residues not originated from the template are refined using the OPLS-2005 force field [27] and a surface Generalized Born continuum solvation model was applied. Structural discontinuities are also repaired. The residue numbers of the template were preserved. The side chains of rotamers for conserved residues were retained. The refinement of the model was achieved using the OPLS3 force field [27]. All the loops of the model were refined using the variable-dielectric generalized Born model (VSGB) [24]. A Ramachandran plot was generated in order to validate the model.

#### Peptides construction and optimization

All the peptides were built in linear conformations using Maestro 10.2 (Schrodinger Suite 2015.2) [28]. The structures were minimized using the OPLS3 force field and, subsequently, they were ionized at a target pH of 7.4 using the LigPrep utility [29].

### Identification of the binding site

SiteID (SYBYL 8.0 [30]), was used in order to identify potential binding sites. This application uses a flood-fill solvation technique during which potential hydrogen bonds are found and the solvent accessible surface area is calculated [31]. The Find Pocket mode was used in combination with the grid method. A grid resolution of 1 Å was chosen with a protein film depth of 3 Å. The residues surrounding the cavity found in this step were used as the center for the generation of the receptor grid in the next step.

### Receptor grid generation

The receptor grid generation was built in Glide 6.7 [32]. The van der Waals radii scaling factor was set at 1.0 with a partial charge cutoff of 0.25 in order to soften the potential of non-polar parts of the receptor [33]. A grid suitable for peptide docking was generated consisting of the following residues: Ser-344, Leu-349, Tyr-350, Tyr-353, His-336, Leu-333, His-255, Val-354, and Leu-357, as identified by SiteID.

### Peptide docking

Numerous applications for flexible protein-peptide docking [34] exist, like CABS-Dock [35], or FlexPepDock [36]. However, since the peptides used in this study contain modified residues, the best available protocol was Glide SP-Peptide [37]. During the standard precision peptide docking, 100,000 poses are kept in the first stage of docking [37]. The top 100 of these poses were refined by a minimization using VSGB2.0, an implicit solvent model. The default van der Waals ligand atom scaling factor of 0.8 was used during the docking [33].

### Induced fit docking

The structures of the three small molecules that act as PAR-4 antagonists (YD-3, ML-354 and BMS-986120) were built in Maestro 10.2 and were minimized using LigPrep [29]. The conformational analysis of the structures was achieved using ConfGen. The resulting conformations were submitted as starting geometries for the Induced Fit Docking calculations with implicit membrane [38,39,24]. At the initial stage of docking, side chains of residues that are within 5 Å of the site as defined by the residues found by SiteID were trimmed. Five residues that are within 5 Å of the ligand and have the highest B-factors (above 40) were refined using Prime 4.0 [24]. The ligands were redocked using the extra precision mode. The implicit membrane is a low-dielectric slab-shaped region, which is treated in the same way as the high-dielectric implicit solvent region. Hydrophobic groups, which normally pay a solvation penalty for creating their hydrophobic pocket in the high dielectric region, do not pay the same penalty while in the membrane slab. Conversely, hydrophilic groups lose any short ranged solvation energy from the high dielectric region when moving into the low dielectric region. The implicit membrane model is intended for use with proteins that span the membrane like PAR-4.

## Results

### Effect of peptides on platelet aggregation

Among all peptides studied, peptide (1) exhibited the most potent platelet aggregatory effect with an EC<sub>50</sub> value of 26.2  $\mu\text{M}$  (Table I). Importantly, Ala-1 for *trans-cinnamoyl*-1 substitution, peptide (7), completely abolishes the agonistic activity of peptide



Figure 1. (A) Representative bar graphs of the effect of 1000  $\mu\text{M}$  *trans*-cinnamoyl-YPGKF-NH<sub>2</sub>, denoted as *tcY* (or its vehicle; DMSO), or 1.25  $\mu\text{M}$  vorapaxar (maximum dose), denoted as Vor (or its vehicle; DMSO), on 100  $\mu\text{M}$  AYPGKF-NH<sub>2</sub> (denoted as AY)-induced platelet aggregation (B) Representative bar graphs of the effect of 0.01  $\mu\text{M}$  vorapaxar (threshold concentration), or its vehicle; DMSO, or 1000  $\mu\text{M}$  *trans*-cinnamoyl-YPGKF-NH<sub>2</sub> (or its vehicle; DMSO), on 10  $\mu\text{M}$  TRAP-6 (denoted as TR)-induced platelet aggregation. All the values are means  $\pm$  SD, obtained from at least three different platelet preparations (\* $P < 0.001$ , compared to 100  $\mu\text{M}$  AYPGKF-NH<sub>2</sub>; \*\* $P = 0.004$ , compared to 10  $\mu\text{M}$  TRAP-6; \*\*\* $P = 0.046$ , compared to 10  $\mu\text{M}$  TRAP-6).

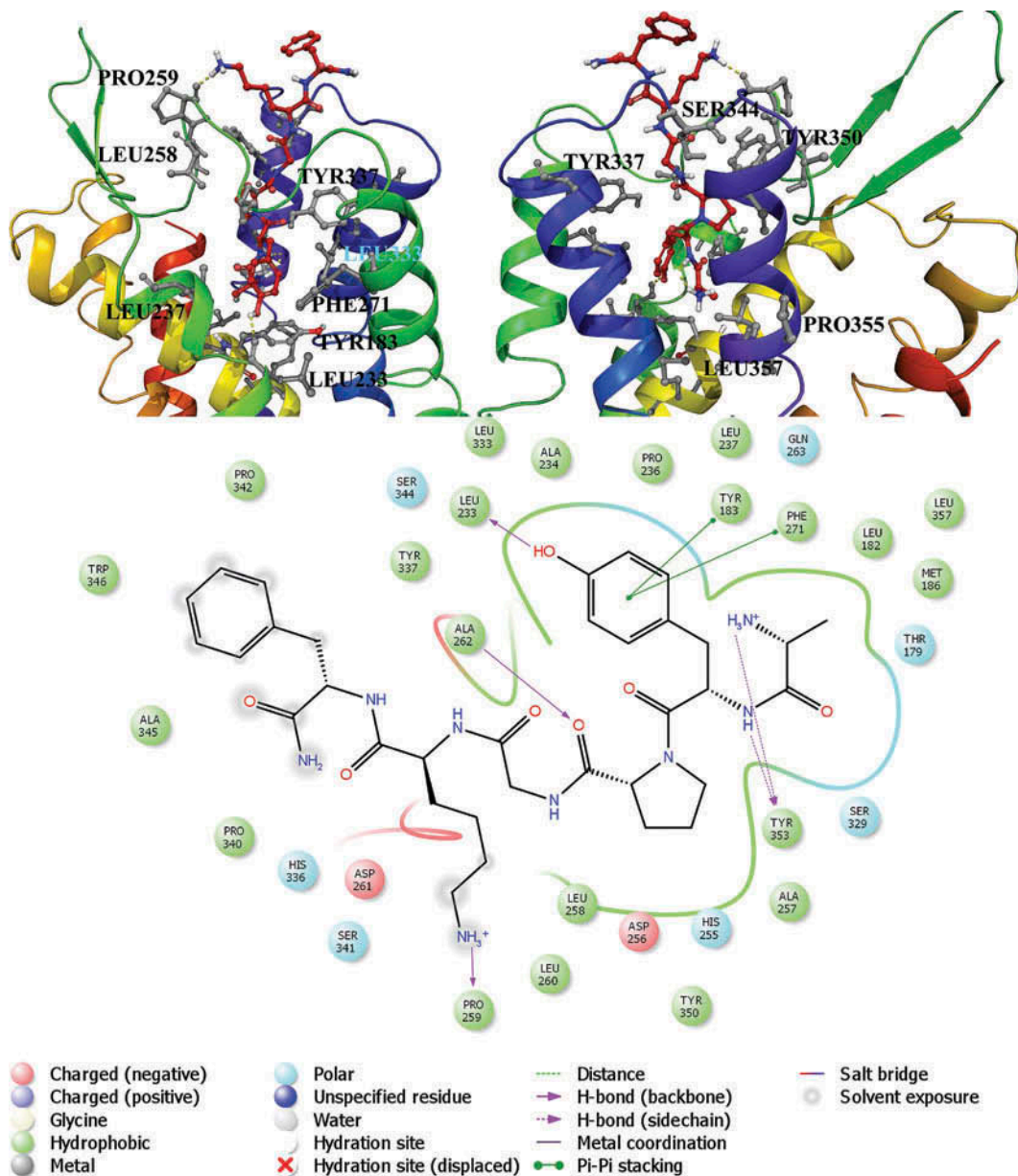
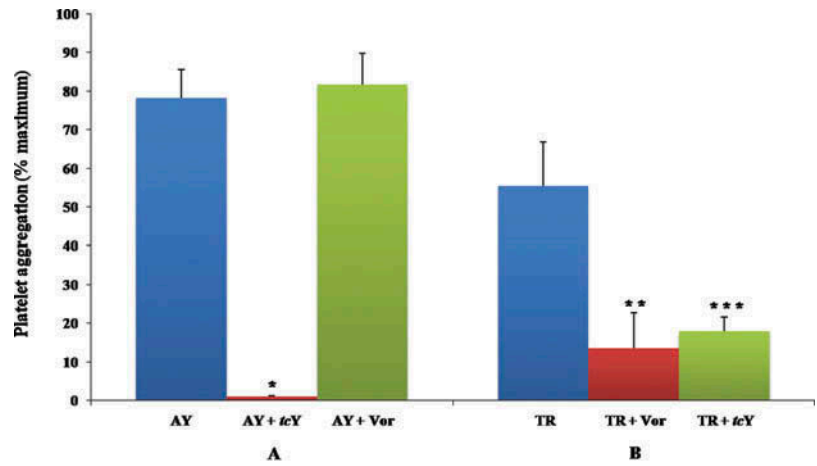


Figure 2. Predicted binding mode for the peptide AYPGKF-NH<sub>2</sub>. The peptide is shown in red.

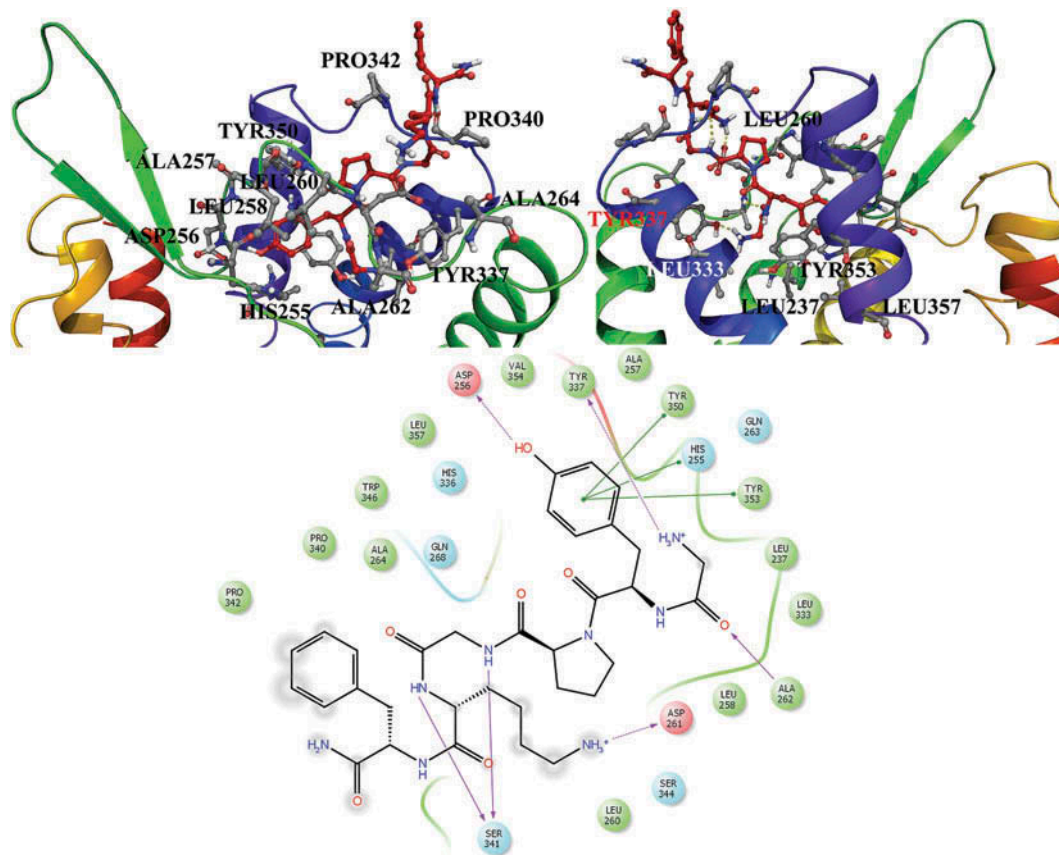


Figure 3. Predicted binding modes for the peptide GYPGKF-NH<sub>2</sub>.

(1) and renders this peptide with a potent antagonistic activity toward peptide (1)-induced platelet aggregation (Table I). All experiments were performed in at least three different platelet preparations.

#### Selectivity of peptides toward PAR-4 and PAR-1

In order to evaluate whether peptide (1) is selective for PAR-4 and it does not exhibit any cross-reactivity with PAR-1, the selective PAR-1 antagonist vorapaxar was used as a reference compound. As expected, vorapaxar potently inhibited TRAP-6-induced platelet aggregation (Figure 1) exhibiting an IC<sub>50</sub> value of 5.7 nM. By contrast vorapaxar, even at a high concentration of 1.25 μM, did not inhibit peptide (1)-induced platelet aggregation (Figure 1). The platelet activating effect of peptide (1) was significantly inhibited by peptide (7) (Figure 1) exhibiting an IC<sub>50</sub> value of 69.4 μM (Table I). Importantly, peptide (7) also significantly inhibited platelet aggregation induced by TRAP-6 albeit to a lesser extent compared with platelet aggregation induced by peptide (1) (Figure 1).

#### In silico studies

As it is shown in Supplementary Figure S1, the primary structure of PAR-1 and PAR-4 illustrate a medium sequence identity (33%) (preserved residues are shown in red). The BLAST bit score for the alignment with PAR-1 was 313 while the second best alignment score was with the crystal structure of the angiotensin II type 1 receptor (PDB ID 4YAY [40]) (BLAST bit score: 297). The Ramachandran plot (Figure S1B) of the modeled receptor pinpoints that most residues are in the favorable region, nine residues are in the allowed region while only four residues are in the disallowed region (Gly-171, Ser-265, Arg-248, Arg-307).

SiteID identified two neighboring cavities (Figure S2 in white and green) that can serve as a binding site for the peptide. The residues surrounding the first cavity (green) are Ser-344, Leu-349, Tyr-350, Tyr-353, Leu-333, and His-336 while the residues surrounding the second cavity (white) are His-255, Arg-158, Leu-357, Leu-182, Val-354, and Tyr-353. The volume of the two sites is 20 and 14 Å<sup>3</sup>, respectively.

#### Docking of the peptides in the PAR-4 homology model

Figures 2–4 and Figures S3–S7 show the predicted binding modes for the peptides: AYPGKF-NH<sub>2</sub>, GYPGKF-NH<sub>2</sub>, *trans*-cinnamoyl-YPGKF-NH<sub>2</sub>, *caffeoyl*-YPGKF-NH<sub>2</sub>, YPGKF-NH<sub>2</sub>, *Ac*-YPGKF-NH<sub>2</sub>, *Ac*-AYPGKF-NH<sub>2</sub>, and *trans*-cinnamoyl-AYPGKF-NH<sub>2</sub>. Two-dimensional and three-dimensional poses are depicted in order to develop a thorough understanding on the interactions of the peptides with the PAR-4 homology model. As it can be observed from the poses, an array of interactions could be recorded for all peptides with the PAR-4 homology model, namely hydrogen bonds, hydrophobic and π-π stacking. Furthermore the poses with best Induced Fit scores for the antagonists YD-3, ML-354 and BMS-986120 are shown in Figure 5 while the ligand interactions diagrams are shown in detail in Figures S8, S9, and S10. The residues involved in the binding are shown in Table II.

#### Discussion

In the present study, we synthesized eight peptide analogues of the tethered-ligand of PAR-4 and evaluated their agonistic/antagonistic potency and selectivity toward platelet aggregation, in order to explore the molecular determinants implicated in the mechanism of activation of this receptor.





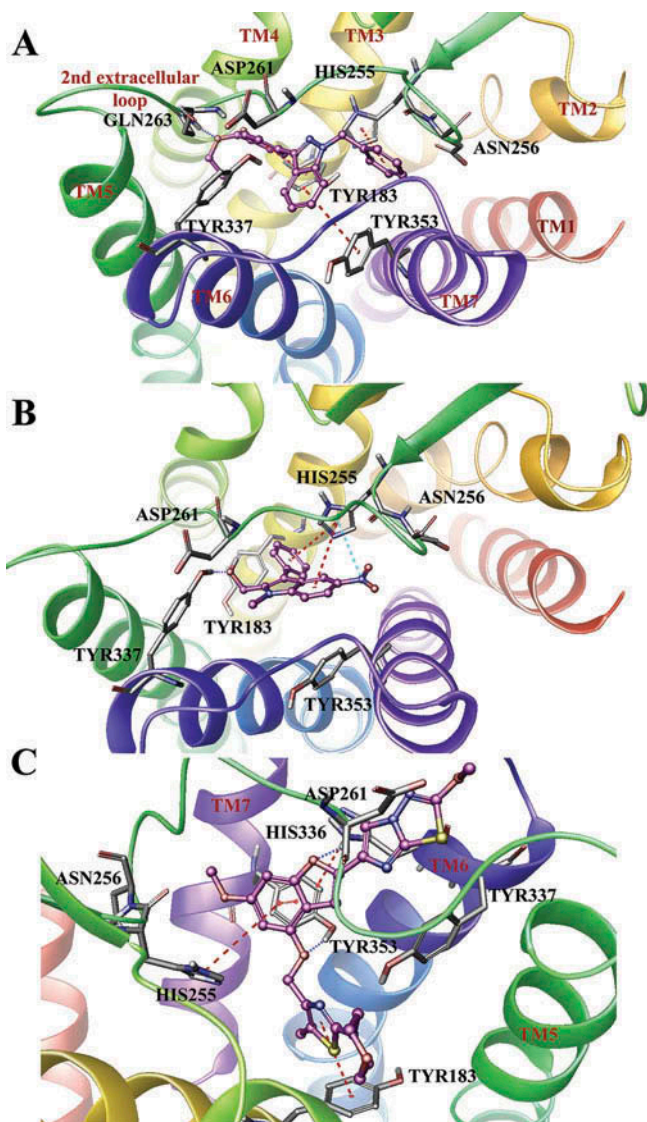


Figure 5. Predicted binding poses of (A) YD-3, (B) ML-354, and (C) BMS-986120. The small molecules are shown in purple while the residues are shown in gray color.

adopting the best Glide SP score allow determining potential common structural features. The most important motif for these inactive peptides is the inability of Tyr-2 to enter inside the transmembrane binding cavity but rather to orient toward the extracellular loops (Figures S3–S7). Phe-6 enters inside the cavity and forms mostly  $\pi$ - $\pi$  interactions with Tyr-183. Other interactions such as hydrogen bonds with residues His-336, His-255, Tyr-353, and Asp-256 amino acids are also eminent.

To further validate the architectural features potentially shared among the different inactive studied peptides and known PAR-4 antagonists, we conducted on the PAR-4 model docking studies of YD-3, ML-354, and BMS-986120, three known PAR-4 antagonists (Figures 5A–C and S8, S9, and S10). The three compounds developed  $\pi$ - $\pi$  stacking with the residues Tyr-183, His-255, and Tyr-353. The compounds ML-354 and BMS-986120 developed further  $\pi$ - $\pi$  stacking interactions with the residues Tyr-337 and His-336 (Table II). The compound YD-3 forms a hydrogen bond with Gln-263 while ML-354 developed one with Tyr-337. ML-354 developed a salt bridge between the negatively charged nitro group and His-255. A superposition of the three compounds with the *trans*-cinnamoyl-YPGKF-NH<sub>2</sub> peptide illustrated several common features (Figure S11). In YD-3 (Figures 5A and S11A) the

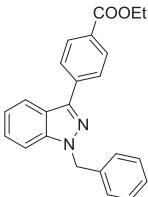
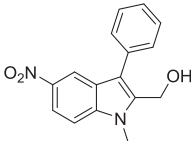
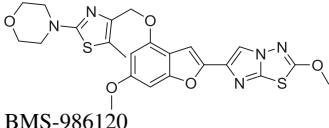
aromatic rings of the compound tend to occupy the same space as the *trans*-cinnamoyl-moiety and the Tyr-2 residue of the peptide. Both the small molecules and the peptide interact with residues such as Tyr-183, Asp-261, His-255, Tyr-353, and Gln-263. The same happens in the cases of ML-354 (Figures 5B and S11B) and BMS-986120 (Figures 5C and S11C). Common interacting residues include Tyr-183, His-255, Asp-256, Tyr-337, and Asp-261. Common  $\pi$ - $\pi$  interactions were observed for the three molecules and the antagonist peptide for Tyr-183. Other  $\pi$ - $\pi$  interactions were observed for aminoacids in spatial vicinity (His-253 and His-255 as well as Tyr-350 and Tyr-353).

A comparison between the binding properties of vorapaxar in the PAR-1 crystal structure and the predicted poses of the small organic and peptidic molecules that act as antagonists in the PAR-4 homology model, shows similarities and differences. The small organic compounds and the peptidic molecules that act as PAR-4 antagonists bind very close to the extracellular surface of the receptor, in a very similar way with vorapaxar's binding to PAR-1. An important difference between the 2 receptors is the substitution of residues Leu-262 and Leu-263 in the second extracellular loop of PAR-1 with Ala and Gln in PAR-4 [25]. Although these residues are not responsible for the selectivity of vorapaxar toward PAR-1, their extensive interactions can influence the binding mode of the drug. In the predicted binding pose of YD-3, Gln-263 develops a hydrogen bond with the compound (Figures 5A and S8) while in the cases of ML-354 and BMS-986120, Ala-262 and Gln-263 are in the vicinity of the predicted binding site. Similarly, in the recently crystallized structure of the angiotensin II type 1 receptor (a GPCR) with olmesartan [44], the second extracellular loop plays a very important role in the binding of the drug, which develops multiple hydrogen bonds with the residue Arg-167 [45]. Another difference between PAR-4 and PAR-1 concerns the third extracellular loop which is one residue shorter in PAR-4 than in PAR-1. As a result, Tyr-337 of PAR-1 forms a strong hydrogen bond with vorapaxar, while in PAR-4 it forms mainly  $\pi$ - $\pi$  interactions with the active small peptides. Similarly, the residues Tyr-353 and Tyr-183 of PAR-1, form the base of the vorapaxar binding pocket, while in PAR-4 they develop mainly  $\pi$ - $\pi$  interactions with its antagonists. The complex of vorapaxar with PAR-1 does not provide any information on how the receptor agonist peptide gains access to its binding site. This is mainly caused by the fact that vorapaxar is a very lipophilic molecule and may enter the PAR-1 active site through the lipid bilayer through a two-step mechanism [25,46] in a similar way that sphingosine-1-phosphate approaches its receptor [47,48]. A comparison between the predicted binding modes of the peptides that act as PAR-4 agonists or antagonists and the crystallized structure of neurotensin receptor-1 (a GPCR) with the peptide agonist NTS<sub>8-13</sub>, shows that in the case of PAR-4 the active peptides are in contact with superficial receptor areas [48].

In conclusion, the lipophilicity, the size and aromatic nature of the residue preceding Tyr-2 is decisive on whether the peptide will be a PAR-4 agonist or antagonist or it will be inactive. Replacement of Ala-1 with Gly-1 reduces the peptide agonistic activity probably because of the different way the peptide is bound to the receptor. When preceding residue Tyr-2 are moieties like the *caffeoyl*- or *acetyl*-roup, Tyr-2 does not enter in the binding cavity. The same happens when Ala and Gly are not preceding the residue Tyr-2. The *trans*-cinnamoyl-moiety enters inside the transmembrane binding cavity and develops more extensive hydrophobic and  $\pi$ - $\pi$  interactions than that of AYPGKF-NH<sub>2</sub>. These extra interactions could be the reason for the antagonistic activity of *trans*-cinnamoyl-YPGKF-NH<sub>2</sub> toward AYPGKF-NH<sub>2</sub>-induced platelet aggregation through PAR-4.



Table II. Predicted interactions of the peptides and small molecules that act as antagonists with PAR-4.

Peptide number	Structure	Hydrogen bonds	Hydrophobic interactions	$\pi$ - $\pi$ interactions
(1)	AYPGKF-NH <sub>2</sub>	Ser-344, 2x Tyr-355, Ala-262, Leu-233, Pro-259	Tyr-337, Ala-257, Tyr-350, Leu-258, Leu-333, Leu-357, Met-186, Leu-182, Leu-237, Pro-236, Ala-234, Pro-340, Pro-342, Trp-346, Ala-345	Tyr-183, Phe-271
(2)	GYPGKF-NH <sub>2</sub>	Asp-261, Asp-256, Tyr-337, Ala-262	Ala-264, Leu-260, Leu-258, Leu-237, Leu-333, Ala-257, Leu-357, Val-354, Pro-340, Pro-342, Trp-346	Tyr-353, His-255, Tyr-350
(3)	Ac-AYPGKF-NH <sub>2</sub>	Asp-261, Tyr-350, His-336, Ser-344, His-255, Tyr-353, Asp-256	Pro-342, Leu-260, Phe-271, Ala-234, Leu-233, Pro-236, Leu-237, Ala-262, Leu-357, Leu-258, Val-354, Ala-257, Leu-333, Pro-340, Tyr-337, Ala-264, Pro-259, Ala-345	Tyr-183
(4)	<i>trans</i> -cinnamoyl-AYPGKF-NH <sub>2</sub>	His-336, Ser-344, Asp-256, His-255, Leu-258, Asp-261	Ala-264, Trp-267, Leu-233, Ala-234, Tyr-183, Pro-236, Ala-262, Ala-237, Phe-271, Leu-333, Val-354, Leu-357, Ala-257, Tyr-353, Pro-340, Leu-332, Tyr-350, Tyr-350, Leu-260, Pro-259, Ala-345, Pro-342	
(5)	YPGKF-NH <sub>2</sub>	Tyr-350, Asp-261, Tyr-353, His-255, His-336, Ser-344 Asp-256	Ala-345, Pro-342, Pro-236, Leu-237, Leu-233, Ala-234, Phe-271, Ala-262, Leu-182, Val-354, Ala-257, Leu-357, Leu-258, Pro-340, Leu-333, Tyr-337, Ala-264, Leu-260, Pro-259	Tyr-183
(6)	Ac-YPGKF-NH <sub>2</sub>	Tyr-353, Ser-344, His-336, His-255	Ala-264, Leu-258, Ala-257, Val-354, Tyr-350, Ala-262, Pro-236, Leu-237, Ala-234, Leu-233, Leu-182, Leu-357, Leu-333, Tyr-337, Leu-260, Ala-345, Pro-342, Pro-340	Tyr-183, Phe-271
(7)	<i>trans</i> -cinnamoyl-YPGKF-NH <sub>2</sub>	Gln-268, Ala-262, Ser-341, 2x Asp-261	Pro-259, Pro-269, Leu-233, Leu-333, Phe-271, Ala-234, Pro-236, Leu-237, Leu-357, Leu-258, Leu-349, Ala-257, Val-354, Tyr-353, Leu-332, Pro-342, Tyr-337, Ala-264, Pro-340, Leu-260, Ala-345	Tyr-183, His-255, Tyr-350
(8)	<i>caffeoyl</i> -YPGKF-NH <sub>2</sub>	His-255, Tyr-353, His-336, Pro-342	Pro-340, Ala-264, Leu-237, Tyr-337, Pro-236, Leu-233, Ala-234, Ala-262, Phe-271, Leu-333, Leu-258, Tyr-350, Leu-357, Val-354, Ala-257, Ala-345, Leu-260, Trp-346	Tyr-183
-		Gln-263	Ala-262, Ala-234, Leu-237, Pro-236, Leu-233, Phe-271, Ala-275, Leu-332, Tyr-337, Leu-333, Leu-357, Val-354, Ala-257, Tyr-350, Leu-258, Leu-260	Tyr-183, His-255, Tyr-353
-		Tyr-337	Leu-357, Met-186, Leu-182, Leu-237, Ala-262, Phe-271, Leu-333, Tyr-350, Val-354, Ala-257	2x His-255, Tyr-353, Tyr-183, Tyr-337
-		-	Tyr-350, Ala-257, Leu-333, Leu-233, Phe-271, Leu-237, Ala-234, Pro-236, Leu-182, Leu-357, Met-186, Ala-262, Pro-340, Ala-264, Val-354, Leu-258	Tyr-353, His-255, Tyr-337, His-336, Tyr-183

Small organic molecules known to exert PAR-4 antagonistic activity can interact at the same binding site as that with the studied peptides and *trans*-cinnamoyl-YPGKF-NH<sub>2</sub> in particular. In addition, they display identical  $\pi$ - $\pi$  interactions with the critical residue Tyr-183, Tyr-353, and His-255. This is an important finding as it sets up the spatial requirements for antagonistic activity. The synthesis of new peptides, peptidomimetic analogs and small organic molecules as well as mutagenesis studies will shed more light on the accurate spatial requirements for activity.

### Acknowledgments

M. Sakka, S. Papadaki, and N. Beckas are acknowledged toward their participation on the initial stages of the project.




### Declaration of interest

The authors report no conflicts of interest.

### Supplemental data

Supplemental data for the article can be accessed on the publisher's website at [www.tandfonline.com/iplt](http://www.tandfonline.com/iplt)

### ORCID

T. F. Kellici  <http://orcid.org/0000-0001-6977-9946>  
 T. Mavromoustakos  <http://orcid.org/0000-0001-5309-992X>  
 A. G. Tzakos  <http://orcid.org/0000-0001-6391-0288>

### References

1. Davey MG, Lüscher EF. Actions of thrombin and other coagulant and proteolytic enzymes on blood platelets. *Nature* 1967;216:857–858.
2. Coughlin SR. Protease-activated receptors in hemostasis, thrombosis and vascular biology. *J Thromb Haemost* 2005;3:1800–1814.
3. Kahn ML, Nakanishi-Matsui M, Shapiro MJ, Ishihara H, Coughlin SR. Protease-activated receptors 1 and 4 mediate activation of human platelets by thrombin. *J Clin Invest* 1999;103:879–887.

4. Vu TK, Hung DT, Wheaton VI, Coughlin SR. Molecular cloning of a functional thrombin receptor reveals a novel proteolytic mechanism of receptor activation. *Cell* 1991;64:1057–1068.
5. Scarborough RM, Naughton MA, Teng W, Hung DT, Rose J, Vu TK, Wheaton VI, Turck CW, Coughlin SR. Tethered ligand agonist peptides. Structural requirements for thrombin receptor activation reveal mechanism of proteolytic unmasking of agonist function. *J Biol Chem* 1992;267:13146–13149.
6. Faruqi TR, Weiss EJ, Shapiro MJ, Huang W, Coughlin SR. Structure-function analysis of protease-activated receptor 4 tethered ligand peptides. Determinants of specificity and utility in assays of receptor function. *J Biol Chem* 2000;275:19728–19734.
7. Leger AJ, Jacques SL, Badar J, Kaneider NC, Derian CK, Andrade-Gordon P, Covic L, Kuliopulos A. Blocking the protease-activated receptor 1-4 heterodimer in platelet-mediated thrombosis. *Circulation* 2006;113:1244–1254.
8. Arachiche A, Mumaw MM, de la Fuente M, Nieman MT. Protease-activated receptor 1 (PAR1) and PAR4 heterodimers are required for PAR1-enhanced cleavage of PAR4 by  $\alpha$ -thrombin. *J Biol Chem* 2013;288:32553–32562.
9. de la Fuente M, Nieman M. Thrombin induces protease-activated receptor 1 and PAR4 heterodimers. *Arterioscler Thromb Vasc Biol* 2012;32:Abstract A56.
10. Covic L, Gresser AL, Kuliopulos A. Biphasic kinetics of activation and signaling for PAR1 and PAR4 thrombin receptors in platelets. *Biochemistry* 2000;39:5458–5467.
11. Moschonas IC, Goudevenos JA, Tselepis AD. Protease-activated receptor-1 antagonists in long-term antiplatelet therapy. Current state of evidence and future perspectives. *Int J Cardiol* 2015;185:9–18.
12. Hollenberg MD, Saifeddine M. Proteinase-activated receptor 4 (PAR4): Activation and inhibition of rat platelet aggregation by PAR4-derived peptides. *Can J Physiol Pharmacol* 2001;79:439–442.
13. Hollenberg MD, Saifeddine M, Sandhu S, Houle S, Vergnolle N. Proteinase-activated receptor-4: Evaluation of tethered ligand-derived peptides as probes for receptor function and as inflammatory agonists in vivo. *Br J Pharmacol* 2004;143:443–454.
14. Ma L, Perini R, McKnight W, Dickey M, Klein A, Hollenberg MD, Wallace JL. Proteinase-activated receptors 1 and 4 counter-regulate endostatin and VEGF release from human platelets. *Proc Natl Acad Sci USA* 2005;102:216–220.
15. Lee FY, Lien JC, Huang JL, Huang TM, Tsai SC, Teng CM, Wu CC, Cheng FC, Kuo SC. Synthesis of 1-benzyl-3-(5'-hydroxymethyl-2'-furyl)indazole analogues as novel antiplatelet agents. *J Med Chem* 2001;44:3746–3749.
16. Wen W, Young SE, Duvernay MT, Schulte ML, Nance KD, Melancon BJ, Engers J, Locuson CW, Wood MR, Daniels JS, Wu W, Lindsley CW, Hamm HE, Stauffer SR. Substituted indoles as selective protease activated receptor 4 (PAR-4) antagonists: Discovery and SAR of ML354. *Bioorg Med Chem Lett* 2014;24:4708–4713.
17. Banville J, Remillard R, Ruediger EH, Deon DH, Gagnon M, Dube L, Guy J, Priestly ES, Posy S, Maxwell BD, Wong PC. Preparation of imidazothiadiazole derivatives and analogs for use as protease activated receptor 4 inhibitors. WO2013163279A1, 2013.
18. Fields GB and Noble RL. Solid phase peptide synthesis utilizing 9-fluorenylmethoxycarbonyl amino acids. *Int J Pept Protein Res* 1990;35:161–214.
19. Sarin VK, Kent SB, Tam JP, Merrifield RB. Quantitative monitoring of solid-phase peptide synthesis by the ninhydrin reaction. *Anal Biochem* 1981;117:147–157.
20. Stathopoulos P, Papas S, Sakka M, Tzakos AG, Tsikaris V. A rapid and efficient method for the synthesis of selectively S-Trt or S-Mmt protected Cys-containing peptides. *Amino Acids* 2014;46:1367–1376.
21. Gkourogianni A, Egot M, Koloka V, Moussis V, Tsikaris V, Panou-Pomonis E, Sakarellos-Daitsiotis M, Bachelot-Loza C, Tsoukatos DC. Palmitoylated peptide, being derived from the carboxyl-terminal sequence of the integrin  $\alpha$ IIb cytoplasmic domain, inhibits talin binding to  $\alpha$ IIb $\beta$ <sub>3</sub>. *Platelets* 2014;25:619–627.
22. Mustard JF, Perry DW, Ardlie NG, Packham MA. Preparation of suspensions of washed platelets from humans. *Br J Haematol* 1972;22:193–204.
23. UniProt Consortium. UniProt: A hub for protein information. *Nucleic Acids Res* 2015;43:D204–212.
24. Schrödinger Release 2015-2: Prime, version 4.0, Schrödinger, LLC, New York, NY, 2015.
25. Zhang C, Srinivasan Y, Arlow DH, Fung JJ, Palmer D, Zheng Y, Green HF, Pandey A, Dror RO, Shaw DE, et al. High-resolution crystal structure of human protease-activated receptor 1. *Nature* 2012;492:387–392.
26. Jacobson MP, Pincus DL, Rapp CS, Day TJJ, Honig B, Shaw DE, Friesner RA. A hierarchical approach to all-atom protein loop prediction. *Proteins: Struct Funct Bioinform* 2004;55:351–367.
27. Shivakumar D, Williams J, Wu Y, Damm W, Shelley J, Sherman W. Prediction of absolute solvation free energies using molecular dynamics free energy perturbation and the OPLS force field. *J Chem Theory Comput* 2010;6:1509–1519.
28. Schrödinger Release 2015-2: Maestro, version 10.2, Schrödinger, LLC, New York, NY, 2015.
29. Schrödinger Release 2015-2: LigPrep, version 3.4, Schrödinger, LLC, New York, NY, 2015.
30. SYBYL 8.0, Tripos International, 1699 South Hanley Rd., St. Louis, Missouri, 63144, USA.
31. Ho CM, Marshall GR. Cavity search: an algorithm for the isolation and display of cavity-like binding regions. *J Comput Aided Mol Des* 1990;4:337–354.
32. Small-Molecule Drug Discovery Suite 2015-2: Glide, version 6.7, Schrödinger, LLC, New York, NY, 2015.
33. Friesner RA, Banks JL, Murphy RB, Halgren TA, Klicic JJ, Mainz DT, Repasky MP, Knoll EH, Shelley M, Perry JK, et al. Glide: A new approach for rapid, accurate docking and scoring. 1. Method and assessment of docking accuracy. *J Med Chem* 2004;47:1739–1749.
34. London N, Raveh B, Schueler-Furman O. Modeling peptide-protein interactions. *Methods Mol Biol* 2012;857:375–398.
35. Kurcinski M, Jamroz M, Blaszczyk M, Kolinski A, Kmiecik S. CABS-dock web server for the flexible docking of peptides to proteins without prior knowledge of the binding site. *Nucleic Acids Res* 2015; 43(W1): W419–W424.
36. London N, Raveh B, Cohen E, Fathi G, Schueler-Furman O. Rosetta FlexPepDock web server—high resolution modeling of peptide-protein interactions. *Nucleic Acids Res* 2011; 39(Web Server issue): W249–W253.
37. Tubert-Brohman I, Sherman W, Repasky M, Beuming T. Improved docking of polypeptides with Glide. *J Chem Inf Model* 2013;53:1689–1699.
38. Small-Molecule Drug Discovery Suite 2015-2: Schrödinger Suite 2015-2 Induced Fit Docking protocol; Glide version 6.7, Schrödinger, LLC, New York, NY, 2015; Prime version 4.0, Schrödinger, LLC, New York, NY, 2015.
39. Sherman W, Day T, Jacobson MP, Friesner RA, Farid R. Novel procedure for modeling ligand/receptor induced fit effects. *J Med Chem* 2006;49:534–553.
40. Zhang H, Unal H, Gati C, Han GW, Liu W, Zatspein NA, James D, Wang D, Nelson G, Weierstall U, et al. Structure of the Angiotensin receptor revealed by serial femtosecond crystallography. *Cell* 2015;161:833–844.
41. Ma L, Hollenberg MD, Wallace JL. Thrombin-induced platelet endostatin release is blocked by a proteinase activated receptor-4 (PAR4) antagonist. *Br J Pharmacol* 2001;134:701–704.
42. Chung AW, Jurasz P, Hollenberg MD, Radomski MW. Mechanisms of action of proteinase-activated receptor agonists on human platelets. *Br J Pharmacol* 2002;135:1123–1132.
43. London N, Movshovitz-Attias D, Schueler-Furman O. The structural basis of peptide-protein binding strategies. *Structure* 2010;18:188–199.
44. Zhang H, Unal H, Desnoyer R, Han, GW, Patel N, Katritch V, Karnik SS, Cherezov V, Stevens RC. Structural basis for ligand recognition and functional selectivity at angiotensin receptor. *J Biol Chem* 2015;290:29127–29139.
45. Kellici TF, Ntountaniotis D, Liapakis G, Tzakos AG, Mavromoustakos T. The dynamic properties of angiotensin II type I receptor inverse agonists in solution and in the receptor site. *Arab J Chem* 2016;doi: 10.1016/j.arabjc.2016.11.014

46. Kellici TF, Ntountaniotis D, Kritsi E, Zervou M, Zoumpoulakis P, Potamitis C, Durdagi S, Salmas RE, Ergun G, Gokdemir E, et al. Leveraging NMR and X-ray data of the free ligands to build better drugs targeting angiotensin II type 1 G-protein coupled receptor. *Curr Med Chem* 2016;23:36–59.
47. Hanson MA, Roth CB, Jo E, Griffith MT, Scott FL, Reinhart G, Desale H, Clemons B, Cahalan SM, Schuerer SC, et al. Crystal structure of a lipid G protein-coupled receptor. *Science* 2012; 335:851–855.
48. Krumm BE, Grisshammer R. Peptide ligand recognition by G protein-coupled receptors. *Front Pharmacol* 2015;6:article 48.